

Chapter I

Modeling Seismic Impedance with Markov Chains

A stochastic model describing impedance is developed in this chapter. One way of constructing *in situ* impedance logs is by multiplying well logs of sonic velocity and rock density together. Another less expensive method is to map the geological section exposed in a road cut. In either case, a common characteristic of the resulting sequence is the box-car or blocky appearance of the log. Stochastically this means that given a certain rock, say carbonate, there is a high probability that the rock immediately above it in the log is also carbonate. If, on the other hand, a new rock type is encountered, say shale, then the probability of finding the shale does not depend on the knowledge that the old rock type was carbonate. Of course the last observation presumes that the length of sedimentary column under study is sufficiently long, e.g. there is an obvious correlation in rock change in a sand-shale sequence.

A well log records the historical sequence of deposition; so the resulting impedance function, obtained by multiplying sonic velocity by density, represents a *depth* series. A seismogram, however, is recorded as a function of time. Integrating a deconvolved seismogram results in impedance indexed as a *time* series. We have a choice; then, of discretizing impedance as either a function of time or depth, and the resulting stochastic model reflects this choice. We use the stochastic model to aid in seismogram deconvolution and inversion, and therefore view impedance as a time sequence. This, of course, necessitates the conversion of well logs into time functions with the known interval velocity.

A considerable portion of this chapter is devoted to developing properties of the model, especially the Bussgang property. Say a time series undergoes an amplitude distortion in a time-varying instantaneous non-linear device. Then, if the autocorrelation of the input is proportional to the crosscorrelation of the input and output, the process from which the time series was realized is said to be Bussgang. A discussion

on the geophysical significance of Bussgang processes will be delayed until Chapter II.

1.1. Impedance and Reflectivity

A review of the equations relating impedance and reflectivity is in order. From plane wave, normal incidence theory, the reflection coefficient c_k at the k -th interface is computed from the impedances i_k and i_{k+1} via

$$c_k = \frac{i_{k+1} - i_k}{i_{k+1} + i_k} \quad (1.1)$$

Inverting equation (1.1) and solving for the i_k gives

$$i_{k+1} = i_1 \prod_{i=1}^k \left(\frac{1 + c_i}{1 - c_i} \right) \quad (1.2)$$

Next, define z_k as the logarithm of impedance [$\log(\text{imped})$]:

$$z_{k+1} = \ln \left(\frac{i_{k+1}}{i_1} \right) \quad (1.3)$$

With this substitution, equation (1.2) becomes

$$z_{k+1} = \sum_{i=1}^k \ln \left(\frac{1 + c_i}{1 - c_i} \right) \quad (1.4a)$$

A good approximation of equation (1.4a) results by using

$$\ln \left(\frac{1 + c_i}{1 - c_i} \right) = 2c_i + O(c_i^3)$$

Hence, for "small" c , equation (1.4a) becomes

$$z_{k+1} = \sum_{i=1}^k 2c_i$$

$$= z_k + 2c_k \quad (1.4b)$$

Equation (1.4b) gives a linear relationship between z and c .

1.2. *The Stochastic Model of Impedance*

Three examples of impedance logs are shown in Figure 1.1. These logs were supplied by Chevron Oil Field Research Company and are the result of carefully editing sonic velocity and density logs, and then multiplying the two together. The reflectivity log was derived from the impedance log using equation (1.1). The blockiness of the latter log is apparent from the plots.

Another perspective on blockiness is illustrated by plotting scattergrams, x_k vs. x_{k+1} , of reflectivity and $\log(\text{imped})$. Figure 1.2 shows that from a probabilistic point of view, it is much easier to propose a model for $\log(\text{imped})$, because of its striking correlation, than it is for reflectivity.

The degree of blockiness in a well log is proportional to the degree of dependence between *adjacent* rock types. The stochastic model, therefore, must be at least of second order. The actual order depends on the physics of the process, the length of data available for analysis, and the degree of complexity of the model. For the last two reasons, only one lag of memory was retained, and we decided to model impedance as a Markov chain. A brief review of Markov chains follows.

1.3. *Markov Chains*

Many excellent textbooks have been written on Markov chains. One that is especially readable is by Kemeny and Snell (1960). The following notation essentially follows theirs.

A sequence of samples has an underlying probability distribution that is Markov if and only if the probability of obtaining a new sample, given the history of the sequence, depends only on the current sample. The sequence of samples is called a "chain," and the term "state" is

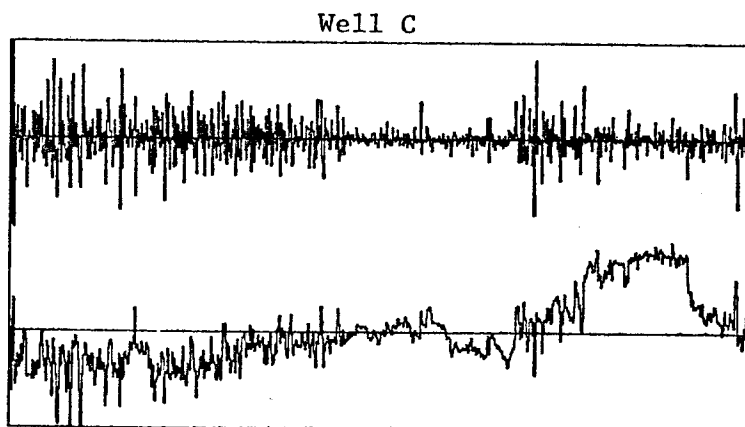
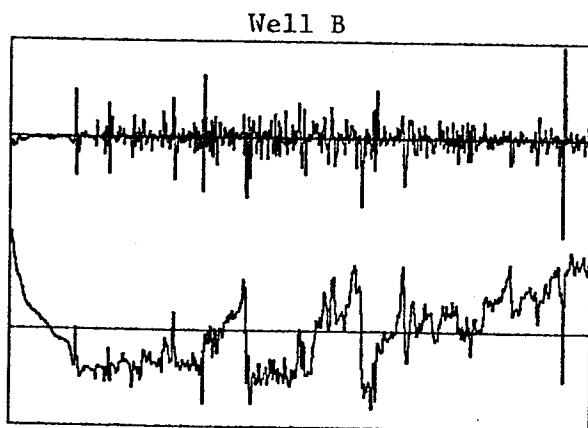
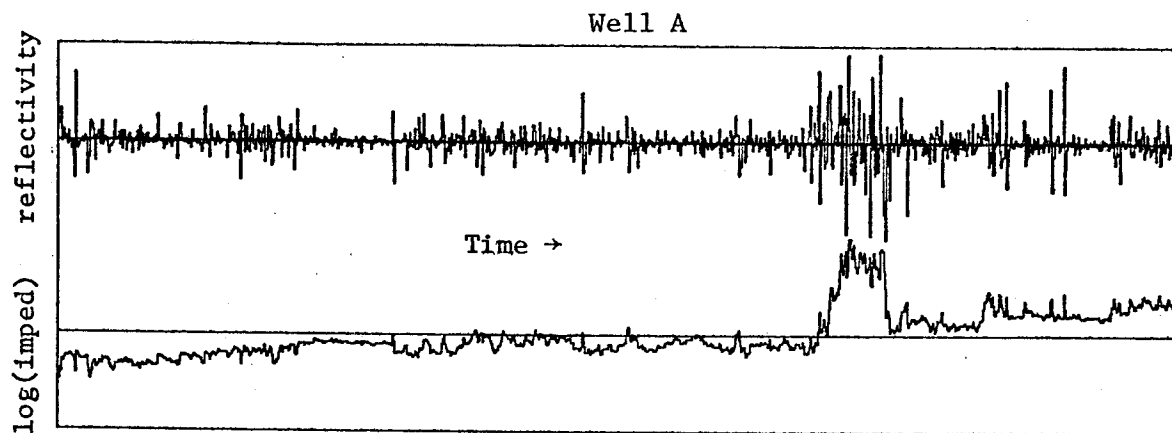


Figure 1.1. Reflectivity and $\log(\text{imped})$ (top and bottom plot in each box) for three wells - A,B,C - provided by Chevron Oil Field Research Company. Number of time samples in Well A = 1153, Well B = 597, Well C = 761.

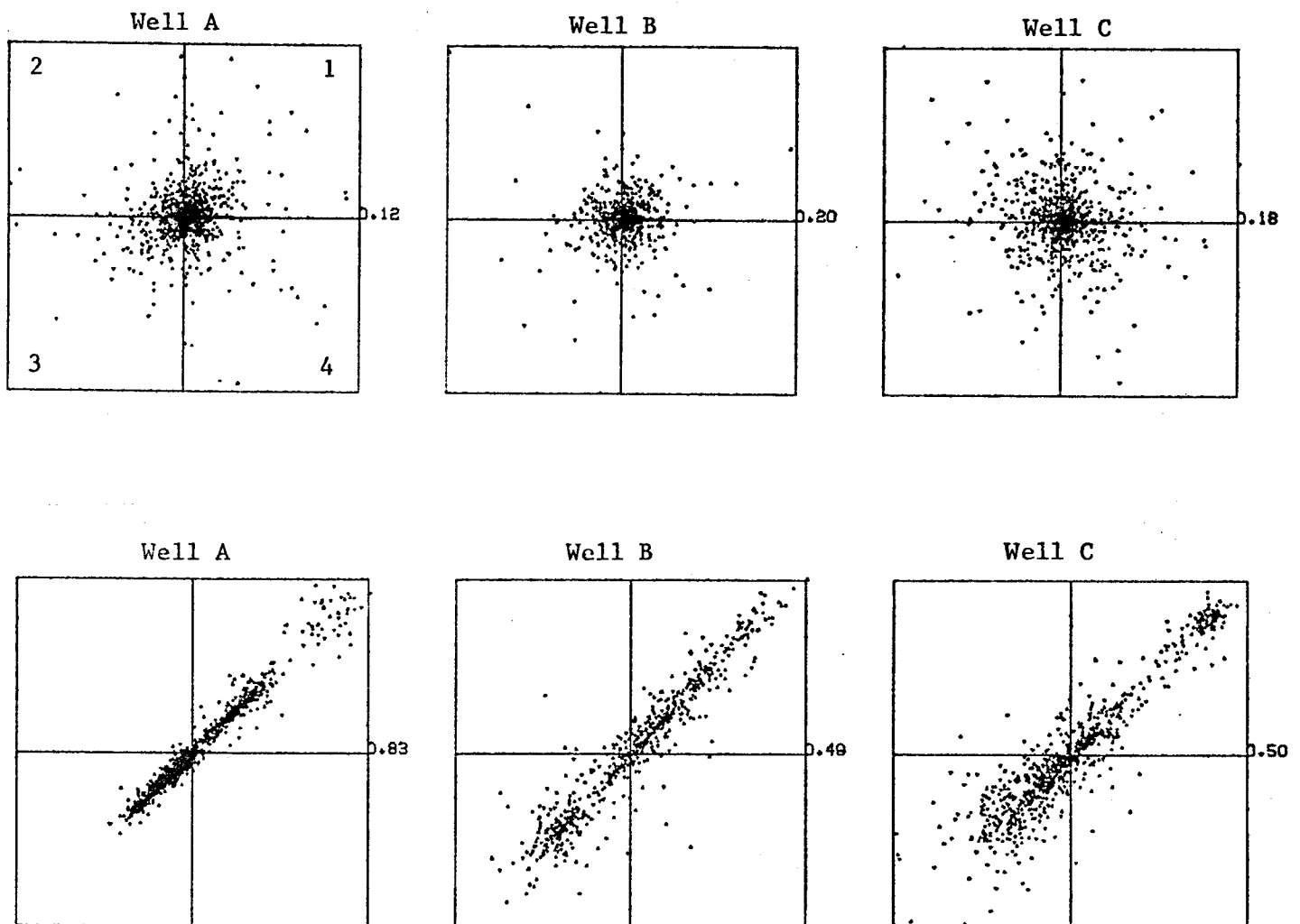


Figure 1.2. *Top row* - Scattergrams of reflectivity for three wells of Figure 1.1. Note the presence of many plus/minus doublets in the second and fourth quadrants, perhaps signifying thin beds. *Bottom row* - Scattergrams of $\log(\text{imped})$ for the three wells of Figure 1.1. The striking correlation (≈ 1 .) suggests using a Markov chain for a stochastic model of impedance.

used in place of "sample." In the case of a sedimentary column, M rock types define M states s_i , $i=1,2,\dots,M$. Note that a state is inherently valueless since any sequence of objects can be broken into states. In our particular situation, we will associate a value of impedance [or $\log(\text{imped})$] with each of the states by constructing the M

component value vector x .

The outcome at any particular time n in the chain is a state s_j , and this statement is written compactly as $Q_n = s_j$, where Q_n is the outcome function at time n . The statement that a sequence is Markov follows:

$$\Pr(Q_n = s_j | Q_{n-1} = s_1, Q_{n-2} = s_h, \dots) = \Pr(Q_n = s_j | Q_{n-1} = s_1) \quad (1.5)$$

where \Pr is short for probability, $0 \leq \Pr \leq 1$. Equation (1.5) introduces the concept of a probability transition matrix (PTM), P , for the chain:

$$\begin{aligned} \{P\}_{ij} &= (i,j) \text{ element of matrix } P = P_{ij} \\ &= \Pr(Q_n = s_j | Q_{n-1} = s_i) \end{aligned} \quad (1.6)$$

$$\sum_j P_{ij} = 1; \quad i = 1, 2, \dots, M$$

Note that the rows of P sum to 1, not the columns. Fixing the row index to $i = 3$, for example, the PTM gives the probability of jumping from s_3 to s_j where j is the current column index. A "blocky" chain would have s_{33} , the largest element in the row.

At the n -th step in a chain, the probability of being in any state is given by the probability state vector π_n . It can easily be shown that

$$\pi_n^T = \pi_{n-1}^T P \quad (1.7a)$$

$$\text{or } \pi_n^T = \pi_0^T P^n \quad (1.7b)$$

$$\sum_i \pi_i = 1$$

Equation (1.7b) is quite remarkable. Essentially, computing P^n keeps track of how many different ways a state at the n -th step can be

initiated from the 0-th step. The probability mass vector α (probability density function for continuous states) is the steady-state solution of equation (1.7a):

$$\alpha^T = \alpha^T P \quad (1.8)$$

A more fundamental matrix than the PTM is the matrix formed from the unconditional probabilities. We call this matrix K for counting matrix:

$$\begin{aligned} \{K\}_{ij} &= K_{ij} = \Pr[Q_n = s_j, Q_{n-1} = s_i] \\ &= \Pr[Q_{n-1} = s_i] \Pr[Q_n = s_j | Q_{n-1} = s_i] \\ &= \alpha_i P_{ij} \\ K &= D P \end{aligned} \quad (1.9)$$

where D is the diagonal matrix with α along the diagonal

$$\begin{aligned} \sum_{ij} K_{ij} &= 1 \\ \sum_j K_{ij} &= \alpha_i \end{aligned} \quad (1.10)$$

We consider K to be the fundamental matrix of Markov chains because both α and P can be calculated from K via (1.10) and (1.9).

Algebraically, it is advantageous to consider the sequence $\{X_k\}$ to be zero mean, where $\{X_k\}$ is shorthand for a sequence of random variables (RV) and is formed by assigning a value to each state in the chain. If we assume the sequences to be stationary, zero mean implies:

$$\begin{aligned} EX &= \sum_i \Pr(Q_n = s_i) x_i \\ &= \sum_i \alpha_i x_i \end{aligned}$$

$$EX = \alpha^T x = 0 \quad (1.11)$$

Since both probability and impedance are positive, $\alpha^T x > 0$. Negative values for x are possible if $\log(\text{imped})$ is modeled vs. imped . The Markov model is valid in both cases, since logarithm is a one-to-one mapping. With an abuse of notation, let x correspond to the value vector for $\log(\text{imped})$ and constrain the choice of values so that equation (1.11) is satisfied. Much of the analysis in Markov Chain theory [e.g. all of the results derived in Kemeny and Snell (1960)] is accomplished without having to specify a conversion vector. In this aspect, we differ. Most of the significant results in this chapter (e.g. the autocorrelation derivation in Section 1.6) demand the specification of such a vector. Some simple experiments, described next, indicated an appropriate one.

1.4. Synthetic Log Computation

A comparison between the actual logs of Figure 1.1 and those synthesized using a Markov chain approach is shown in Figure 1.3. Before discussing the comparison, the technique used to generate the synthetic logs will be explained.

The original log was quantized into fifteen states. Two different quantization schemes were tried. In the first, the range of impedance values was partitioned into uniform intervals with each interval defining a state. Events were then assigned the states corresponding to the intervals they fell within. The second scheme used quantiles selected from the data to partition the impedance range. Although this scheme resolves small events very well (many small events \rightarrow many states), large events are poorly resolved due to their scarcity. The first scheme resolves all events uniformly and was adopted for this reason.

After quantizing, K is formed:

$$K_{ij} = \frac{\text{number of } s_i - s_j \text{ pairs}}{\text{number of samples}} \quad (1.12)$$

Then, α and P are computed via equations (1.10) and (1.9). To start the chain, a state s_k is chosen from the distribution α (calling a random number generator). The state vector π_0 is then formed by inserting the value 1 at the k -th position in the vector. The new state vector π_1 can then be computed as $\pi_0^T P$ (k -th row of P). As before, a new state s_j is chosen from the distribution π_1 , and the whole procedure is re-started. In this way a synthetic state log is created. The conversion from state to value is accomplished by assigning values from x to the states.

The top plots of Figure 1.3 represents the original log quantized into 15 states. The large number of states has resulted in both large and small-scale features of the original log being retained in the quantized version (compare Figure 1.1). Three synthetics are shown for each original log, and a cursory examination indicates that all synthetics "look" like logs. Of course the stochastic model has 225 degrees of freedom (M^2 , in general) corresponding to the number of elements in K , and it is not surprising that the synthetics mimic the original logs so well. The next two sections are concerned with reducing the degrees of freedom in the model.

1.5. Reversible Chains

Most sedimentary sections are reversible, that is, tops and bottoms are difficult to distinguish. Probabilistically, this means

$$\Pr(Q_n=s_j, Q_{n-1}=s_i) = \Pr(Q_n=s_i, Q_{n-1}=s_j)$$

$$K_{ij} = K_{ji}$$

$$K^T = K$$

In all the counting matrices investigated, $K^T \approx K$. Corresponding elements differ by < 1% on average; hence, constraining K to be symmetric is geologically sound and as a bonus, reduces the degree of freedom in the model from M^2 to $M^2/2$. A first order model, one that

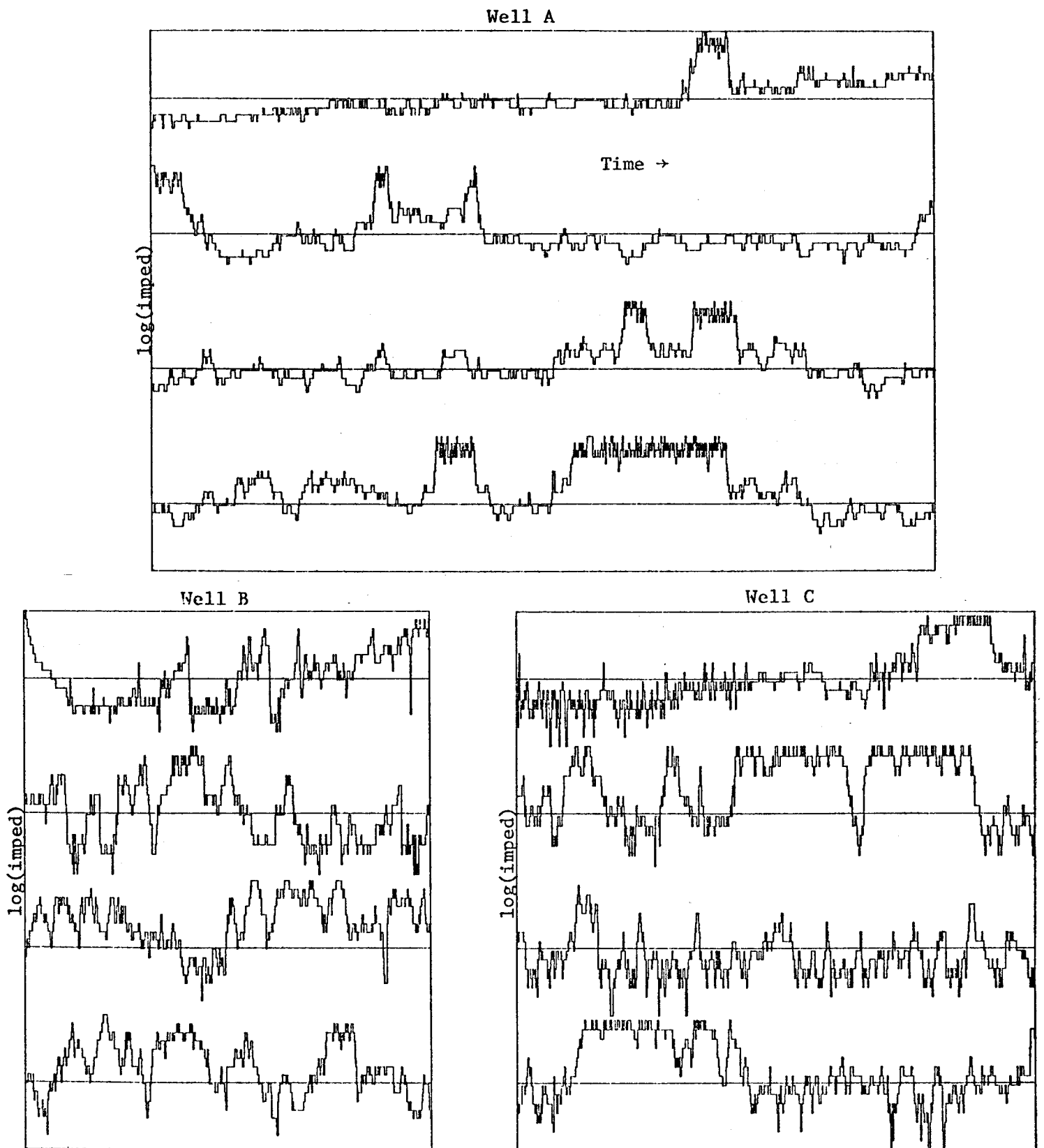


Figure 1.3. The top plot of each group is the original $\log(\text{imped})$ of Figure 1.1 quantized into 15 states. The bottom three plots are synthetics generated using the probability transition matrix derived from the top log. In all cases, both fine-scale and gross features of the quantized logs are preserved in the synthetics.

treats samples independently, is completely specified by $M-1$ parameters, corresponding to the probability mass function. This property sets the lower bound for the number of parameters necessary to describe a second order model at M . We would like to force the K matrix to have only M parameters but in doing so we want to retain the blockiness characteristic of the original process. Correlation is one statistic that certainly reflects the blockiness of a time series, and in the next section an expression for the autocorrelation of a Markov chain is derived.

1.6. Autocorrelation of the Chain

The autocorrelation for the chain $\{X_n\}$ at lag k is computed as follows:

$$\begin{aligned}
 R_{xx}(k) & \triangleq E X_n X_{n+k} \\
 & = \sum_{ij} x_i x_j \Pr(Q_n = s_i, Q_{n+k} = s_j) \\
 & = \sum_{ij} x_i x_j \Pr(Q_n = s_i) \Pr(Q_{n+k} = s_j | Q_n = s_i) \\
 & = \sum_{ij} \alpha_i x_i P_{ij}^k x_j, \text{ where } P_{ij}^k \text{ means } \{P^K\}_{ij} \\
 & = x^T D P^k x \quad (1.13)
 \end{aligned}$$

Using equation (1.13), the autocorrelation for the three quantized logs of Figure 1.1 (top plots in Figure 1.3) were computed and the results plotted in Figure 1.4. A best fit exponential curve is also plotted with the autocorrelation function.

The agreement for large lags is excellent, but for lags close to zero, the exponential lies below the actual curve, indicating the presence of a noise-like component in the actual logs. We call this noise "geological noise," and the reader is referred to the section on the *telegraph matrix* for a further discussion. The exponential is a

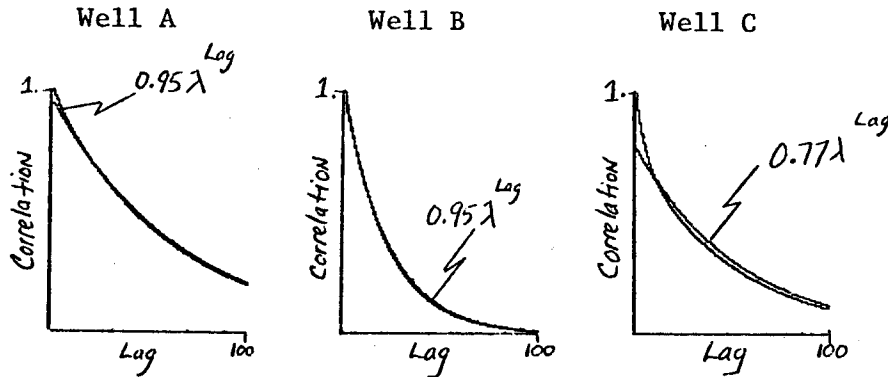


Figure 1.4. Autocorrelation function of the three logs of Figure 1.3 plotted with a best fit exponential. In wells A and B, the curves are indistinguishable except at the origin, where the exponential falls below the actual curve. In Well C, the two curves are distinguishable at all lags. The presence of a noise component on the logs is indicated by the difference in the two curves at the origin. For Well A, $\lambda = 0.98$; Well B, $\lambda = 0.96$; Well C, $\lambda = 0.98$, where λ equals the coefficient of the exponential.

parsimonious description of an autocorrelation function, and we pose the question, how can P (or K) be smoothed so that the correlation is purely exponential? Assuming P has a complete set of eigenvectors, we can decompose it into row and column eigenvectors:

$$P = \sum_{i=1}^M \lambda_i \mu_i \beta_i^T \quad (1.14)$$

$$\mu_i = \text{column eigenvector}$$

$$\beta_i^T = \text{row eigenvector}$$

$$\beta_j^T \mu_i = \delta_{ij}$$

Using (1.14), P^k becomes

$$p^k = \sum_{i=1}^M \lambda_i^k \mu_i \beta_i^T \quad (1.15)$$

Substituting equation (1.15) into equation (1.13) gives

$$R_{xx}(k) = x^T D \sum_{i=1}^M \lambda_i^k \mu_i \beta_i^T x$$

But $\alpha^T x = 0$ (zero-mean process); hence, calling $\beta_1 = \alpha$ gives

$$R_{xx}(k) = x^T D \sum_{i=2}^M \lambda_i^k \mu_i \beta_i^T x \quad (1.16)$$

For equation (1.16) to give a pure exponential decay, there are two alternatives:

$$(a) \quad \lambda_i = \lambda, \quad i = 2, 3, \dots, M$$

$$(b) \quad \lambda_i = \lambda, \quad i = 2, 3, \dots, R$$

$$\lambda_i = 0, \quad i = R+1, R+2, \dots, M$$

In model (a), the exponential will be continuous for all lags, whereas in model (b), a singularity may exist in going from $k = 0$ to $k = 1$. In a subsequent section it is shown that reflectivity functions do indeed have a singularity when going from lag 0 to lag 1 and model (b) is the appropriate one. The small discontinuity in the impedance correlation function at lag 0 would also suggest model (b) for impedance sequences. Theoretically, such a choice causes difficulty and we have been unable to prove that any of the properties that exist for impedance PTMs formed using model (a), hold for impedance PTMs having zero eigenvalues. For this reason model (a) was adopted for impedance and equation (1.16) becomes:

$$R_{xx}(k) = x^T D \lambda^k \sum_{i=2}^M \mu_i \beta_i^T x$$

$$\text{But} \quad I = \sum_{i=1}^M \mu_i \beta_i^T$$

$$\therefore \quad Ix = \sum_1^M \mu_1 \beta_1^T x$$

$$\text{Hence,} \quad R_{xx}(k) = \lambda^k x^T D x \quad (1.17)$$

Therefore, if we force P to have $M-1$ equal eigenvalues, the process will have a purely exponential decay, regardless of what value is assigned to the corresponding state, as long as $\alpha^T x = 0$.

1.7. The Telegraph Matrix P_T

In this section, we describe a class of PTMs having a purely exponential autocorrelation function. We denote these matrices by P_T ; the choice of subscript will be apparent later. P_T is completely specified by only M parameters.

A class of PTMs that have a non-zero eigenvalue repeated $M-1$ times is given by the construction,

$$P_T = \lambda I + (1 - \lambda) \Gamma \alpha^T \quad (1.18)$$

Γ = column vector of ones

λ = only eigenvalue of P_T not equaling 1

Proof:

We have to show that (i) α^T is a row eigenvector of eigenvalue 1 and (ii) λ is an eigenvalue repeated $M-1$ times.

$$\begin{aligned} \text{(i)} \quad \alpha^T P_T &= \lambda \alpha^T + (1 - \lambda) \alpha^T \Gamma \alpha^T \\ &= \alpha^T (\alpha^T \Gamma = 1), \quad \text{Q.E.D.} \end{aligned}$$

$$\text{(ii)} \quad \beta_i^T P_T = \lambda \beta_i^T + (1 - \lambda) \beta_i^T \Gamma \alpha^T$$

There are $M-1$ vectors β_i , which can be chosen perpendicular to Γ , hence:

$$\beta_i^T P_T = \lambda \beta_i^T ; \quad i = 2, \dots, M$$

From this we conclude that λ is repeated $M-1$ times. Q.E.D.

Equation (1.18) is easily interpreted if the matrices involved are written out explicitly:

$$P_T = \lambda \begin{bmatrix} 1 & & & \\ & 1 & & \\ & & 1 & \\ & & & \ddots \\ & & & & 1 \end{bmatrix} + (1 - \lambda) \begin{bmatrix} \alpha^T \\ \alpha^T \\ \alpha^T \\ \alpha^T \end{bmatrix} \quad (1.19)$$

Assume we are in state k . The parameter λ is interpreted as the bias of a coin (biased toward heads). If the result of a coin toss is heads, we stay in state k ; otherwise we have an opportunity to change states. The matrix $\Gamma \alpha^T$ represents an independent process since all rows are identical. If the coin toss results in tails, we choose a new state, independent of the previous state. It is quite possible to select state s_k again (especially if α_k is ≈ 1) and the effect is to remain in state s_k . In terms of rocks, this means that at an unconformity, a sand overlies a sand. The independence of $\Gamma \alpha^T$ means the transition from a sand to shale is as likely as a transition from carbonate to shale, given that an unconformity exists. This description is much like a random telegraph signal when $M=2$; hence, the subscript (T) in P_T , which we call the *telegraph matrix*.

The corresponding counting matrix K_T is

$$\begin{aligned} K_T &= DP_T \\ &= \lambda D + (1 - \lambda) \alpha \alpha^T \end{aligned} \quad (1.20)$$

From (1.20) we conclude that K_T is symmetric; hence, the chains are reversible.

The coefficient of the best-fit exponential is chosen for the value

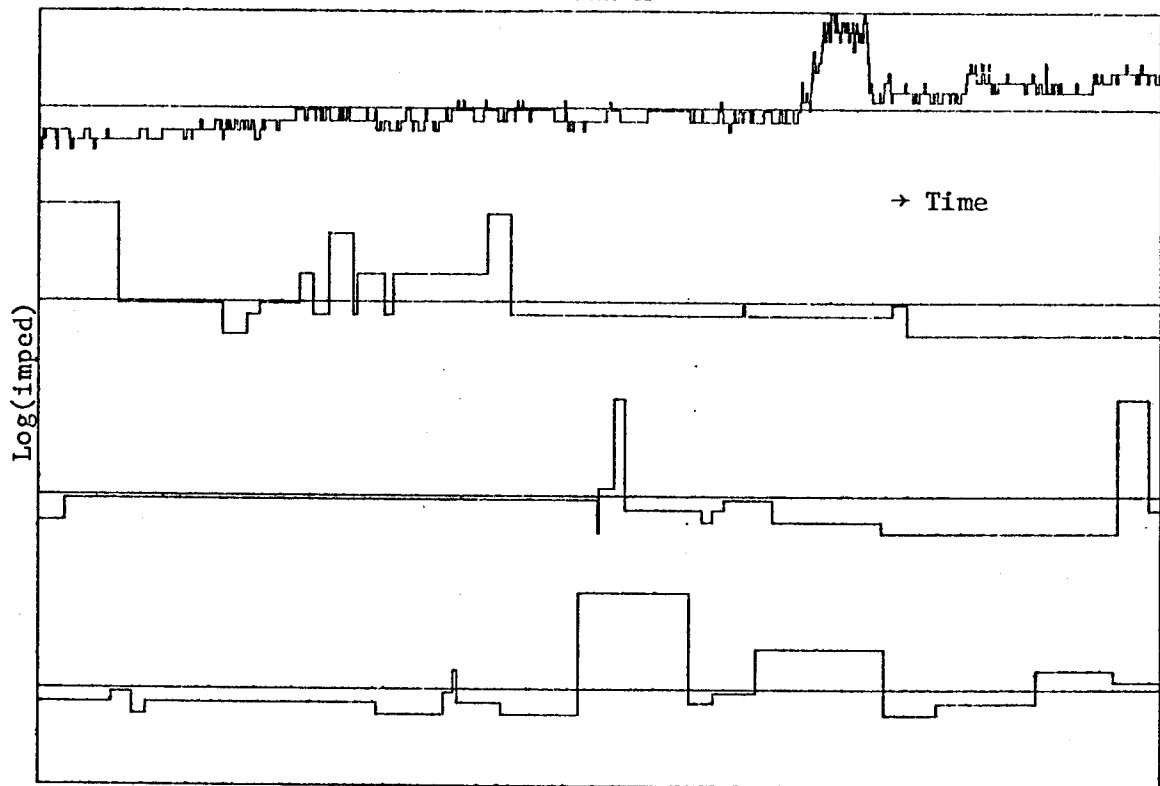
of λ , which is regarded as a measure of blockiness. Since λ is an eigenvalue of a PTM, it has a range: $-1 < \lambda \leq 1$. A value of $\lambda = 1$ indicates a chain that never changes state and hence is perfectly blocky. An independent process is represented by $\lambda = 0$, and the corresponding chain has no tendency to be blocky since it is uncorrelated. Negative values of λ indicate a chain that is quite erratic, with a desire to jump out of the current state. While it is hard to imagine an impedance log having $\lambda < 0$, an argument can be made for reflectivity logs having negative values.

The probability mass vectors for both PTMs, P and P_T , are identical. Coupled with the value of λ , chosen by the above method, the M parameters of P_T are completely specified.

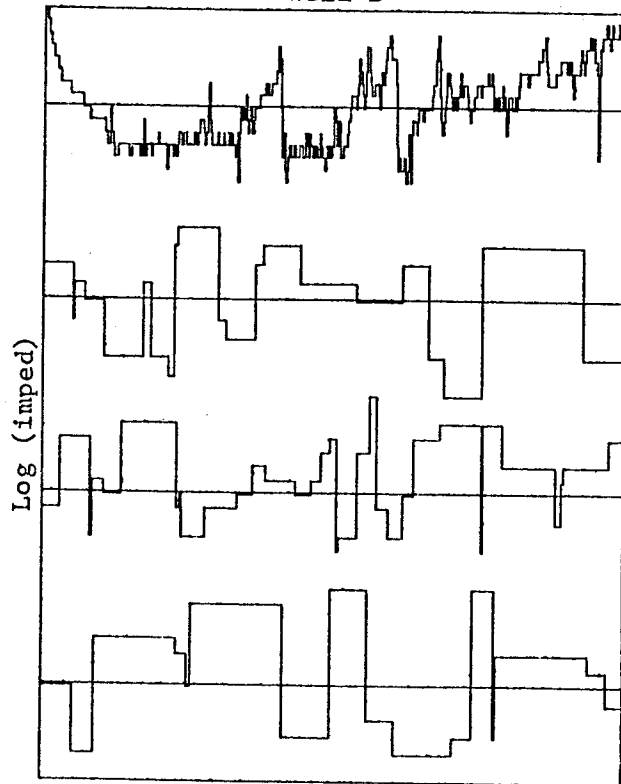
When M is large, say 15, the difference between chains computed using P and P_T is considerable since P allows small-scale fluctuations that P_T prohibits. This point is illustrated in Figure 1.5 by comparison of the top plot of each group with the synthetic logs computed using P_T . The synthetics can be made to look noisy by adding some "geological noise" onto the P_T chain. This noise, which is independent of the P_T chain, can be either uncorrelated (white) or weakly correlated ($\lambda \approx 0$), and its variance can be computed as the difference in the curves of Figure 1.4 at zero-lag.

In summary, the telegraph matrix is the simplest second order stochastic model of impedance possible. The model cannot simulate all features of impedance logs; it will, however, simulate the blockiness characteristic, which a first order model is incapable of reproducing. The next section discusses the Bussgang property of P_T . Will Gray (1979) noted that variable norm deconvolution converges (in expectation) to reflectivity sequences that are Bussgang. Before studying reflectivity, however, we show that if the PTM characterizing $\log(\text{imped})$ is P_T , then $\log(\text{imped})$ is Bussgang.

Well A



Well B



Well C

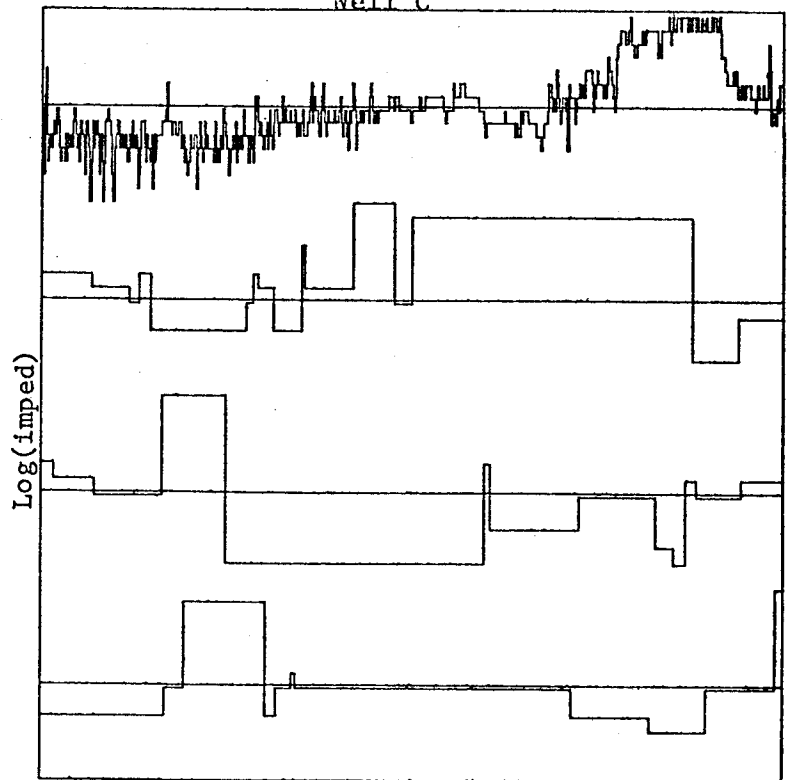


Figure 1.5. The top plots are identical to the top plots of Figure 1.3. The bottom plots are synthetics generated using the telegraph matrix P_T . All fine-scale structure is lost in the synthetics; however, the gross blockiness of the original logs is retained.

1.8. The Bussgang Property of P_T

Consider the process $\{Y_t\}$ formed by passing $\{X_t\}$ through a zero-memory non-linear (ZNL):

$$y_t = \text{ZNL}(x_t) \quad (1.21)$$

The process $\{X_t\}$ has the Bussgang property if and only if

$$\frac{EX_n X_{n+k}}{EX_{n+k} Y_n} = \frac{R_{xx}(k)}{R_{xy}(k)} = \text{constant, all } k \quad (1.22)$$

Restricting the PTM to be of the class P_T , an expression for $R_{xy}(k)$ can be derived in an analagous manner to that which gave equation (1.13):

$$\begin{aligned} R_{xy}(k) &= \sum_{ij} y_i x_j \Pr(Q_{n+k}=s_j, Q_n=s_i) \\ &= \lambda^k y^T D x, \quad k \geq 0 \end{aligned} \quad (1.23)$$

Equation (1.23) is equally valid for negative lags. For instance,

$$\begin{aligned} R_{xy}(-1) &= E X_n Y_{n+1} \\ &= x^T K y \end{aligned} \quad (1.24)$$

Since $R_{xy}(-1)$ is a scalar, transposing equation (1.24) does not change the answer:

$$\begin{aligned} R_{xy}(-1) &= y^T K^T x \\ &= y^T K x = R_{xy}(1) \end{aligned}$$

A similar symmetry argument can be used for all other lags. Hence,

$$R_{xy}(k) = \lambda^{|k|} y^T D x$$

The process $\{X_t\}$ is Bussgang since equation (1.22) holds, i.e.

$$\frac{R_{xx}(k)}{R_{xy}(k)} = \frac{x^T D x}{y^T D x} \neq f(k)$$

1.9. Reflectivity from Impedance

Given two adjacent values of $\log(\text{imped})$, either equation (1.4a) or (1.4b) can be used to calculate reflectivity. In either case, the new chain is constructed by combining adjacent states of the old chain. Figure 1.6 illustrates the construction.

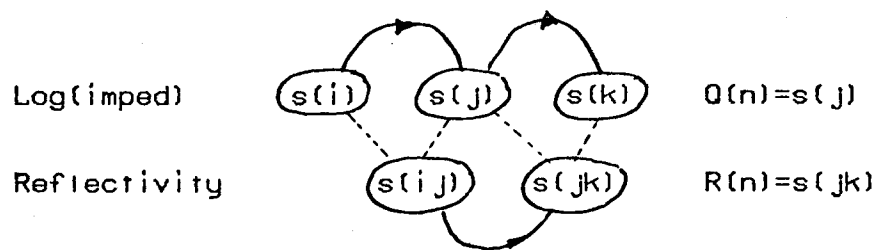


Figure 1.6. Combining adjacent states in the $\log(\text{imped})$ chain produces a new Markov chain of M^2 states -- the reflectivity.

What are the properties of the reflectivity process, given that the $\log(\text{imped})$ process was P_T ? For instance, do differential processes of P_T retain the Bussgang property of P_T , or more fundamentally, are they even Markov? In this section, it will be shown that reflectivity is both Markov and Bussgang. This fact proves that there are at least two equilibrium points for iterative deconvolution algorithms - the reflectivity and $\log(\text{imped})$ sequences. The next chapter discusses this point in detail.

The PTM of the new chain \tilde{P}_T has M^2 states, and is related to

P_T via

$$\begin{aligned}
 \tilde{P}_{(ij).(kl)} &= \Pr[R_n = s_{(kl)} | R_{n-1} = s_{(ij)}] \\
 &= \Pr(Q_n = s_l, Q_{n-1} = s_k | Q_{n-1} = s_j, Q_{n-2} = s_i) \\
 &= \Pr(Q_n = s_l | Q_{n-1} = s_k, Q_{n-2} = s_i) \delta_{jk} \\
 &= \Pr(Q_n = s_l | Q_{n-1} = s_k) \delta_{jk} \\
 &= P_{kl} \delta_{jk} \tag{1.25}
 \end{aligned}$$

Equation (1.25) is proof that the expanded chain inherits the Markov property of the original chain. The corresponding probability mass vector $\tilde{\alpha}$ is constructed from K via

$$\begin{aligned}
 \tilde{\alpha}_{(ij)} &= \Pr[R_n = s_{(ij)}] \\
 &= \Pr(Q_n = s_j, Q_{n-1} = s_i) \\
 &= K_{ij}
 \end{aligned}$$

Figure 1.7 shows the expansion of a three-state chain into a nine-state chain and should clarify the notation used in the above equations. The value vector \tilde{x} is formed by using either equation (1.4a) or (1.4b) together with the original values x . In either case, it is simple to show that

$$\tilde{\alpha}^T \tilde{x} = 0$$

i.e. the new chain is zero-mean. The mapping from state to value is *onto* (not one-to-one). For instance, there are always M zero values corresponding to the M states $s_{(11)}$, $i = 1, 2, \dots, M$. By partitioning the state-space ("lumping states") a mapping that is one-to-one can be effected. The lumped process is no longer Markov, however. For this reason, we retain M^2 states.

$$\begin{aligned}
P_T &= \begin{bmatrix} A & b & c \\ a & B & c \\ a & b & C \end{bmatrix} & \tilde{P}_T &= \begin{bmatrix} A & b & c & 0 & 0 & 0 & 0 & 0 & 0 \\ 0 & 0 & 0 & a & B & c & 0 & 0 & 0 \\ 0 & 0 & 0 & 0 & 0 & 0 & a & b & C \\ A & b & c & 0 & 0 & 0 & 0 & 0 & 0 \\ 0 & 0 & 0 & a & B & c & 0 & 0 & 0 \\ 0 & 0 & 0 & 0 & 0 & 0 & a & b & C \\ A & b & c & 0 & 0 & 0 & 0 & 0 & 0 \\ 0 & 0 & 0 & a & B & c & 0 & 0 & 0 \\ 0 & 0 & 0 & 0 & 0 & 0 & a & b & C \end{bmatrix} \\
K_T &= \begin{bmatrix} d & e & f \\ e & g & h \\ f & h & i \end{bmatrix} & \tilde{\alpha} &= [d \ e \ f \ e \ g \ h \ f \ h \ i]
\end{aligned}$$

Figure 1.7. The original chain, characterized by the PTM P_T and counting matrix K_T is expanded into M^2 states, giving \tilde{P}_T and $\tilde{\alpha}$.

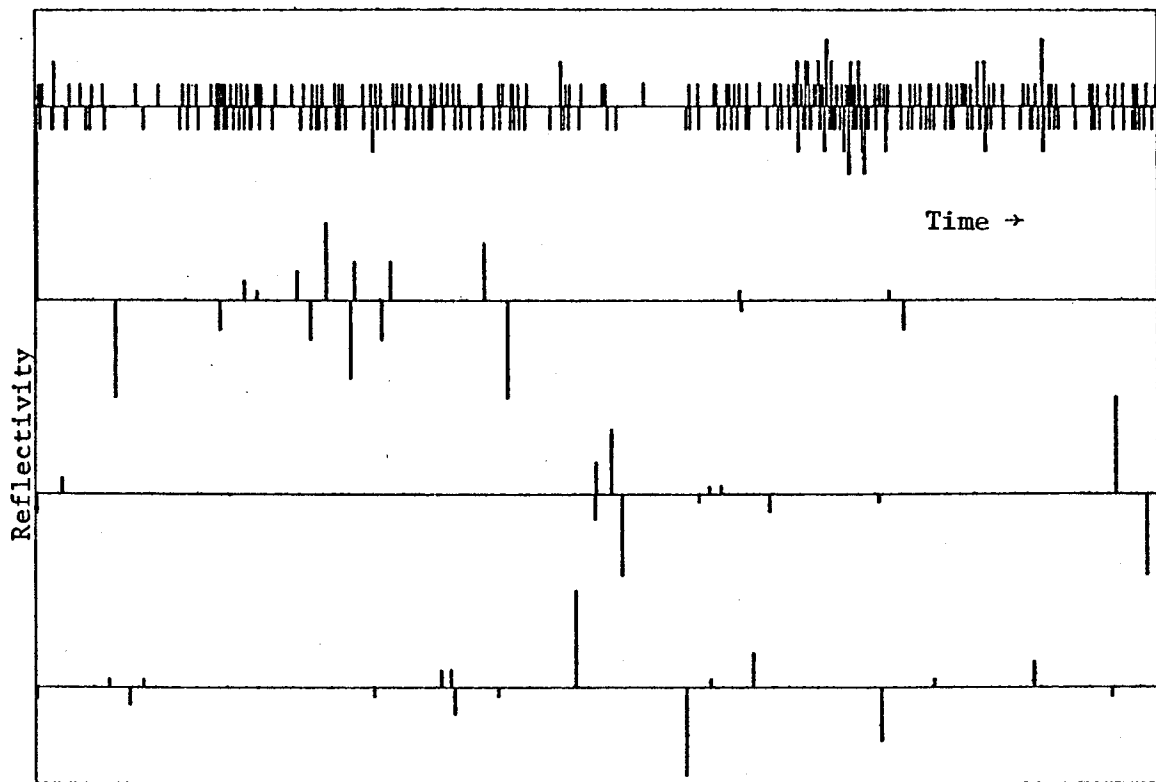
While theoretically advantageous, the PTM \tilde{P}_T has dimensions ($M^2 \times M^2$) that quickly exhaust core storage in a computer. For this reason, we computed synthetic reflectivity sequences (Figure 1.8) by applying equation (1.4b) (differentiating) directly to the synthetic $\log(\text{impd})$ logs of Figure 1.5. The reasons for choosing equation (1.4b) over (1.4a) will become apparent in the next section. As expected, the actual reflectivity sequence (top figure) is much "noisier" than the synthetic sequences.

The remainder of this chapter is concerned with establishing the Bussgang property of the reflectivity sequences.

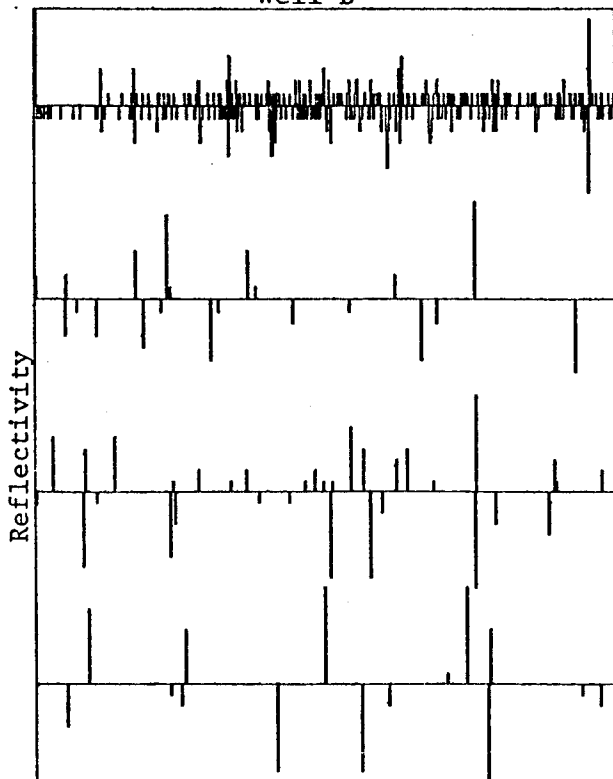
1.10. The Bussgang Property of \tilde{P}_T

Previously, it was shown that chains constructed using P_T exhibit the Bussgang property. Are the reflectivity sequences computed using \tilde{P}_T also Bussgang? To answer this, we first derive an expression for the autocorrelation.

Well A



Well B



Well C

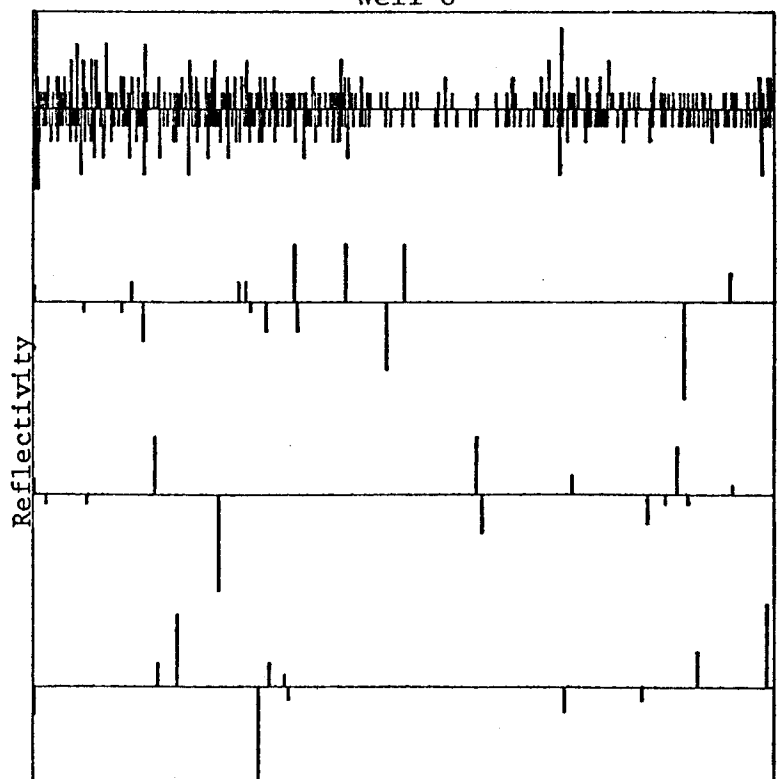


Figure 1.8. All plots are the differentiated versions of Figure 1.5. As expected, the synthetics (bottom three plots) contain fewer reflection coefficients than the actual reflectivity sequence (top plot).

Denoting reflectivity by C_k , a random variable, equation (1.4b) relates C_k to a differential process involving X_k [a random variable representing $\log(\text{imped})$]:

$$C_k = X_k - X_{k-1} \quad (1.26)$$

The autocorrelation of C is

$$\begin{aligned} R_{cc}(j,k) &= E C_j C_k \\ &= E[(X_j - X_{j-1})(X_k - X_{k-1})] \end{aligned} \quad (1.27)$$

From equation (1.17), however, we have an expression for the autocorrelation of X :

$$R_{xx}(t) = \lambda^{|t|} \quad \text{where } x^t \text{ is } \Delta \times 1 \quad (1.28)$$

Expanding equation (1.27) and substituting equation (1.28) gives

$$\begin{aligned} R_{cc}(0) &= 1 \\ R_{cc}(t) &= - \left(\frac{1 - \lambda}{2} \right) \lambda^{|t|-1}, \quad |t| > 0 \end{aligned} \quad (1.29)$$

where the zero-lag has been normalized to one. The values of λ corresponding to the three chains of Figure 1.8 were substituted into equation (1.29) and the results are plotted at the top of Figure 1.9. The actual autocorrelation of the reflectivity sequences of Figure 1.1 is plotted at the bottom of Figure 1.9. The small negative values at lag one in Figure 1.9, top row, indicate that reflectivity is very weakly correlated, so a valid probabilistic model could treat reflectivity as an independent process. The empirical autocorrelation (Figure 1.9, bottom row), however, has a much larger negative value at lag one, indicating a dependent process, or failure of the telegraph model. The reason for this discrepancy is two-fold. First, the actual reflectivity sequence has many plus/minus doublets that are absent on the synthetic logs. Second, the presence of white noise in the $\log(\text{imped})$ process

will give anticorrelated noise in the differential process. Note that the derivation leading up to equation (1.29) assumes a purely differential process, and for this reason, equation (1.4b) was adopted.

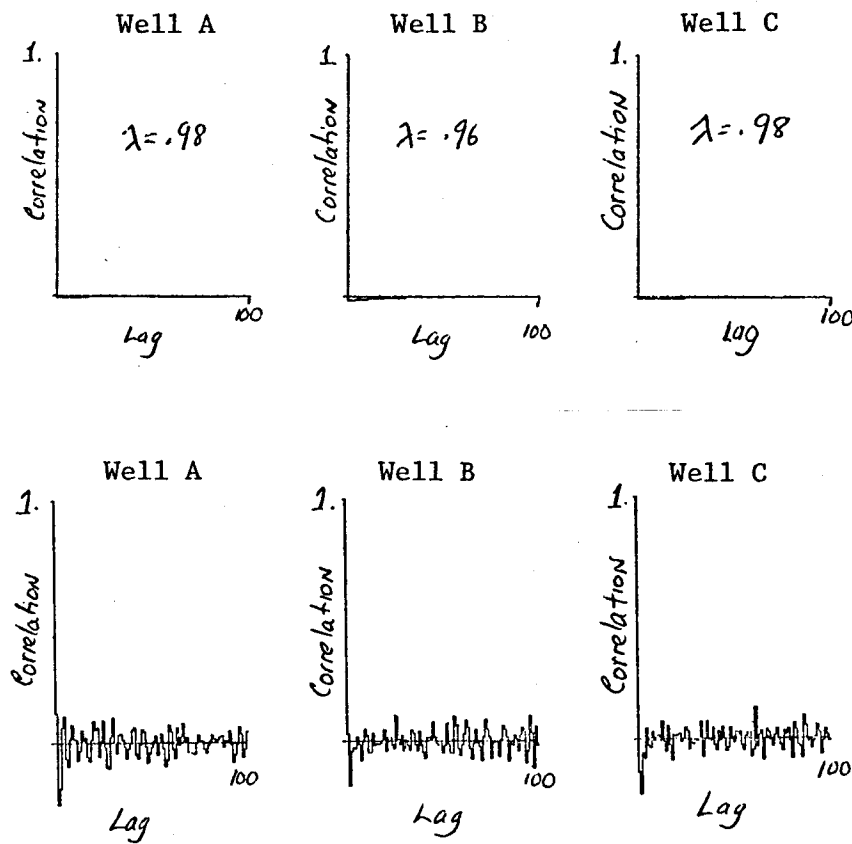


Figure 1.9. *Top row* - The theoretical autocorrelation function of the three logs of Figure 1.8. based on the telegraph assumption. The negative values for lags ≥ 1 are hardly visible since $[(\lambda - 1)/2] \approx 0$. One might conclude that reflectivity is an independent process on the basis of these plots. *Bottom row* - The sample correlation function of the reflectivity sequences of Figure 1.1. Note the large negative pulse at lag 1.

To show that $\{C_k\}$ is Bussgang, it is necessary to derive a relation for the crosscorrelation of C_k with a ZNL. The calculation is carried out in an earlier paper (SEP-16, p. 270). If the ZNL is restricted to being odd, for example,

$$y_t = \text{sgn}(x_t) |x_t|^\alpha$$

then $\{C_k\}$ is indeed Bussgang.

1.11. Chapter Summary

We model impedance as a special type of Markov chain, one which is constrained to have a purely exponential correlation function. The stochastic model is parsimoniously described by M parameters, where M is the number of states or rocks composing an impedance well log. The probability mass function of the states provides $M-1$ parameters, and the "blockiness" of the log determines the remaining degree of freedom. Synthetic impedance and reflectivity logs constructed using the Markov model mimic the blockiness of the original logs. Both synthetic impedance and reflectivity are shown to be Bussgang, i.e. if the sequence is input into an instantaneous non-linear device, then the correlation of input and output is proportional to the autocorrelation of the input. This means that iterative deconvolution algorithms have at least two equilibrium points, namely reflectivity and impedance sequences. Whether both of these are *stable* is another matter. The next chapter will explore these latter points further.